Original Article on Narrative & Evidence-based Medicine for Traditional Medicine: from Basic Research to Clinical Practice and Trial

Effect of Tang-Shen-Ning decoction on podocyte epithelial-esenchymal transformation via inhibiting Wnt/β-catenin pathway in diabetic mice

Fang-Qiang Cui[1#], Yan-Bin Gao[2,3#], Yue-Fen Wang[1], Yuan Meng[1], Zhen Cai[1], Cun Shen[1], Xin-Can Jiang[2,3], Wen-Jing Zhao[1]

[1]Department of Nephrology, Beijing Hospital of Traditional Chinese Medicine, Capital Medical University, Beijing, China; [2]School of Traditional Chinese Medicine, Capital Medical University, Beijing, China; [3]Beijing Key Lab of TCM Collateral Disease Theory Research, Beijing, China

Contributions: (I) Conception and design: FQ Cui, WJ Zhao; (II) Administrative support: YB Gao, YF Wang; (III) Provision of study materials or patients: Y Meng, Z Cai; (IV) Collection and assembly of data: FQ Cui, C Shen, XC Jiang; (V) Data analysis and interpretation: FQ Cui; (VI) Manuscript writing: All authors; (VII) Final approval of manuscript: All authors.

[#]These authors contributed equally to this work.

Correspondence to: Prof. Wen-Jing Zhao. Department of Nephrology, Beijing Hospital of Traditional Chinese Medicine, Capital Medical University, 23 Meishuguanhou Street, Dongcheng District, Beijing 100010, China. Email: wenjingz@263.net.

Background: Diabetic nephropathy (DN) is the leading cause of end-stage renal disease (ESRD). Podocyte epithelial-esenchymal transformation (EMT) induced by the activated Wnt/β-catenin pathway plays a key role in DN. Tang-Shen-Ning (TSN), a Chinese herbal formula, has been shown to decrease proteinuria and protect the renal function in DN. However, the effect of TSN on the Wnt/β-catenin pathway and podocyte EMT is unclear.

Methods: TSN was orally administrated in KK-Ay mice for 4 weeks, at a daily dose of 20 g/kg body weight in our *in vivo* study. Rat serum containing TSN was added in podocyte cultured in high glucose for 24 h. The levels of 24 h urine protein, serum creatinine and blood urea nitrogen were detected by ELISA. Nephrin, Synaptopodin, P-cadherin, desmin, FSP-1, and collagen I protein and mRNA expressions were detected by western blot, immunohistochemistry, immunofluorescence, and RT-PCR. Snail, β-catenin, and TCF/LEF were detected by Western blot, RT-PCR and luciferase.

Results: TSN significantly decreased 24-h urine protein, serum creatinine, and blood urea nitrogen in DN mice. Further, TSN also significantly increased the expression of nephrin, synaptopodin, and P-cadherin, while the expression of desmin, fibroblast-specific protein 1 (FSP-1), and collagen I of podocytes was significantly decreased. Moreover, TSN significantly inhibited the activation of the Wnt/β-catenin pathway in podocytes cultured under high glucose (HG). Notably, the effect of TSN on podocyte EMT was reversed by activation of the Wnt/β-catenin pathway.

Conclusions: TSN could protect podocytes from injury in DN, partly via inhibiting the activation of the Wnt/β-catenin pathway and ameliorating podocyte EMT.

Keywords: Tang-Shen-Ning (TSN); diabetic nephropathy (DN); podocyte; epithelial-esenchymal transformation (EMT); Wnt/β-catenin pathway

Submitted Mar 21, 2020. Accepted for publication Jun 16, 2020.
doi: 10.21037/apm-20-602
View this article at: http://dx.doi.org/10.21037/apm-20-602

Introduction

Diabetic nephropathy (DN), an important microvascular complication of diabetes mellitus (DM), is the leading cause of end-stage renal disease (ESRD) (1); however, the precise underlying mechanisms of DN remains unknown. Previous studies have demonstrated that podocyte injury can induce albuminuria and lead to the progression of DN (2-4). Although the podocyte injury has been a potential therapeutic target for DN in recent years (5), the underlying mechanism of podocyte injury in DN remains unclear.

It has been demonstrated that podocytes undergo a process of epithelial-esenchymal transformation (EMT) in DN (6). Moreover, podocyte EMT can induce changes in podocyte morphology and phenotype, such as actin cytoskeleton rearrangement, slit diaphragm loss, and increased cuboidal morphology (7). Meanwhile, podocytes lose their original phenotype of epithelial cells and acquire some of the mesenchymal characteristics (8). Thus, podocyte EMT plays a critical role in podocyte dysfunction, proteinuria, and glomerulosclerosis in DN. It has been demonstrated that inhibition of podocyte EMT can attenuate albuminuria and other renal injuries related to DN (9). In recent years, the key role of the Wnt/β-catenin signaling pathway in podocyte EMT has been highlighted by many studies (10-12). Therefore, inhibiting the activation of the Wnt/catenin pathway and ameliorating podocyte EMT may be an important potential therapeutic target for DN.

Traditional Chinese medicine (TCM) compounds can include preventive and curative delays in the progression of diabetes and its complications (13-15). TSN formula is an herbal medicine based on the empirical experience of a Chinese medicine expert, Yan-Bin Gao. TSN consists of Chinese herbal medicines, including *Astragalus membranaceus* (*Fisch*.) *Bunge* (Huangqi in Chinese), *Rehmannia glutinosa Libosch* (Shengdi in Chinese), *Euryale ferox Salisb*. *ex DC* (Qianshi in Chinese), *Cornus officinalis* (Shanzhuyu in Chinese), *Rheum palmatum L* (Dahuang in Chinese), and *Ligusticum chuanxiong Hort* (Chuanxiong in Chinese). TSN can provide relief for symptoms manifested by edema, dysuria, and oliguria in DN patients. Moreover, Astragaloside IV, a major active component of TSN, can prevent podocyte EMT in DN (16). However, the effect of TSN on podocyte EMT and the Wnt/β-catenin pathway is unclear.

KK-Ay mice is a kind of a spontaneous animal model of DM. KK-Ay mice has been used as an useful spontaneous animal model for the evaluation of pathogenesis and treatment in patients with type 2 DN in recent years. Thus, KK-Ay mice and cultured podocyte will be used in our *in vivo* and *in vitro* study. The present study will detect the effect of TSN on podocyte EMT and the Wnt/β-catenin pathway in DN mice and in HG cultured podocyte. We present the following article in accordance with the ARRIVE reporting checklist (available at http://dx.doi.org/10.21037/apm-20-602).

Methods

TSN formula preparation

TSN was purchased from the Beijing Hospital of Traditional Chinese Medicine, Capital Medical University. TSN consists of 6 herbs: *Astragalus membranaceus* (*Fisch*.) *Bunge* (Huangqi in Chinese), *Rehmannia glutinosa Libosch* (Shengdi in Chinese), *Euryale ferox Salisb*. *ex DC* (Qianshi in Chinese), *Cornus officinalis* (Shanzhuyu in Chinese), *Rheum palmatum L* (Dahuang in Chinese), and *Ligusticum chuanxiong Hort* (Chuanxiong in Chinese). The six constituent herbs were mixed at a ratio of 6:6:3:3:1:2, respectively. The lyophilized powder of TSN was ground and extracted from the 6 herbs. We obtained 1 g of TSN lyophilized powder from 8.04 g of crude herbs. The quality and substance analysis was performed by high-performance liquid chromatography-electrospray ionization-tandem mass spectrometer (HPLC-ESI-MS^n) analysis. The lyophilized powder of TSN was finally restored at 4 ℃ for further study.

HPLC-ESI-MS^n analysis

HPLC-ESI-MS^n analysis was performed using a Shimadzu UHPLC system (Kyoto, Japan) equipped with an LC-30AD solvent delivery system, an SIL-30AC autosampler, a CTO-30A column oven, a DGU-20A3 degasser, and a CBM-20A controller. A Waters ACQUITY UPLC HSS T3 (21× 100 mm, 1.8 μm) was used for compound separation at 35 ℃. The flow rate of the mobile phase was 0.4 mL/min under a gradient program. The mobile phase consisted of 0.05% formic acid in water (A) and acetonitrile (B). The gradient system was 0–1 min, 2% B; 1–40 min, 2–50% B; 40–53 min, 50–95% B; 53–56 min, 95% B; 56–56.1 min, 95–2% B; and 56.1–60 min, 2% B. The peak intensity was monitored using a diode-array detector at 254 nm. A

TripleTOF 5600+ system with a DuoSpray source (SCIEX, Foster City, CA, USA) was used to acquire the mass spectra in negative and positive electrospray ionization (ESI). The data were analyzed by PeakView Software 2.2 (SCIEX, Foster City, CA, USA).

Animals

Our animal experiment was performed following the National Institutes of Health Guide for the Care and Use of Laboratory Animals. The study was approved by the Medical Ethics Committee of Captical Medical University (No. AEEI-2018-073). Male KK-Ay and C57BL/6J mice, aged 8 weeks and weighing 20–30 g, were purchased from the Chinese Academy of Medical Sciences (Beijing, China). All animals were housed at a constant temperature (24±1 ℃) and humidity (50–60%), with a regular 12-h light and 12-h dark cycle in a specific-pathogen-free (SPF) room. All animals had free access to water. KK-Ay mice were fed high-fat fodder for 4 weeks, while C57BL/6J mice were fed regular fodder. When 24-h urinary protein ≥500 μg, KK-Ay mice were considered DN mice. A total of 20 KK-Ay mice were randomly divided into the DN group and TSN group. A total of 10 C57BL/6J mice were fed as a control in the normal control (NC) group. For statistical analysis, 10 mice were fed in every group. Mice in the TSN group were gavaged with TSN solution at 20 g/kg/d (crude herb). Mice in the NC and DN groups were gavaged normal saline at equal volume. The treatment lasted for 12 weeks. After that, the serum and renal cortices of all mice were collected (*Figure 1*).

Preparation of rat serum containing drug

A total of 28 Sprague Dawley rats were randomly divided into four groups: NC group, low dose TSN group, medium dose TSN group, and high dose TSN group. Rats in TSN group were gavaged with TSN solution at a dose of 5, 10, and 20 g/(kg·d) for 3 days respectively. Meanwhile, rats in the NC group were gavaged with normal saline as the normal control. The serum of all rats was then collected incubated in a water bath for 30 min at 56 ℃. The serum containing the drug was finally stored at –80 ℃.

Cell culture and treatment

The conditionally immortalized mouse podocyte line was used in our *in vitro* study. The podocyte line was obtained from the National Platform of Experimental Cell Resources for Sci-Tech (Beijing, China). The podocytes were cultured in Dulbecco's Modified Eagle Media (DMEM)/low glucose (HyClone, Logan, UT, United States) with interferon gamma (IFN-γ; PeproTech, Rocky Hill, New Jersey, USA) at 33 ℃. Subsequently, podocytes were differentiated in medium without IFN-γ at 37 ℃. When grown to 80% confluence, podocytes were cultured in the medium without fetal bovine serum for 24 h. Podocytes were then divided into five groups: NC group, HG group, TSN group, CTNNB1 knockout ($CTNNB1^{Ko}$) group, and CTNNB1 knockin ($CTNNB1^{Ki}$) group. Podocytes of the NC group were cultured in medium containing 5.5 mmol/L glucose + 24.5 mmol/L mannitol +normal rat serum. Podocytes of HG group were cultured in medium containing 5.5 mmol/L glucose + 24.5 mmol/L glucose + normal rat serum. Podocytes of TSN group were cultured in medium containing 5.5 mmol/L glucose + 24.5 mmol/L glucose + low dose, medium dose, and high dose rat serum of TSN. Podocytes of the $CTNNB1^{Ko}$ group were cultured in medium containing 5.5 mmol/L glucose + 24.5 mmol/L glucose + $CTNNB1^{Ko}$. Podocytes of $CTNNB1^{Ki}$ group were cultured in medium containing 5.5 mmol/L glucose + 24.5 mmol/L glucose + rat serum of TSN + $CTNNB1^{Ki}$.

siRNA transfection

$CTNNB1^{Ko}$ and $CTNNB1^{Ki}$ were procured from Santa Cruz Biotechnology (Santa Cruz, CA, USA). Transfection was conducted using the Lipofectamine 2000 transfection reagent (Invitrogen), according to the manufacturer's protocol. To confirm the transfection, protein expression of β-catenin was detected by Western blot.

Cell counting kit-8 (CCK-8)

Podocytes (10,000 cells/well) were cultured in 96-well plates. Podocyte were culture with serum-free DMEM for 24 h. To detect the cytotoxicity of TSN, podocyte were divided into four groups: NC group (DMEM medium + 10% serum of NC group), NC + low dose TSN group (DMEM medium + 10% serum of low dose TSN group), NC + medium-dose TSN group (DMEM medium + 10% serum of medium-dose TSN group), and NC + high dose TSN group (DMEM medium + 10% serum of high dose TSN group). To detect of TSN on podocyte injury, podocytes were divided into five groups: NC group (DMEM medium + 10% serum of NC group), HG group

Table 1 Sequences of primers

Name	Forward primer (5'-3')	Reverse primer (5'-3')
Nephrin	AATTGGCGGCTGGGTCTTAGGG	AGGCGTGTGGGCGTGTATATGT
P-cadherin	TGTATGGTGGCGGTGAGGATGA	GGATCAGTGTTGTCGTCAGAGTCA
Synaptopodin	AGTGAGGAAGAGGAAGTGCCATTG	GCTGACTGTGGTGACTGCTAGAG
Desmin	AGACCTTCTCTGCTCTCAACTTCC	CTCGCTGACAACCTCTCCATCC
FSP-1	CTGCCCAGATAAGGAGCCC	TGTGCGAAGAAGCCAGAGTAA
Collagen I	TTCCTGCCTCAGCCACCTCAA	GTACTCTCCGCTCTTCCAGTCAGA

(DMEM medium + 24.5 mmol/L glucose + 10% serum of NC group), low dose TSN group (DMEM medium + 24.5 mmol/L glucose + 10% serum of low dose TSN group), medium-dose TSN group (DMEM medium + 24.5 mmol/L glucose + 10% serum of medium-dose TSN group), and high dose TSN group (DMEM medium + 24.5 mmol/L glucose + 10% serum of high dose TSN group). All treatments lasted for 24 h. Subsequently, podocytes were incubated with 10 μL CCK-8 solution for 2 h at 37 ℃. The optical density (OD) of each well was detected at 450 nm using a spectrophotometer.

Hematoxylin and eosin (HE), Masson, and periodic acid-Schiff (PAS) staining

Renal tissue was fixed by 4% paraformaldehyde solution. Subsequently, renal tissue was embedded in paraffin and 4 μm thin slices were sectioned. Renal tissue was then stained by H-E, PAS solution, and Masson three-color staining, respectively. The sections were observed with a fluorescent microscope.

Western blot (WB) analysis

A lysis buffer was added to the renal cortex and collected podocytes and lysis was performed on ice for 30 min. The lysed tissues were centrifugated and protein was extracted. Extracted protein was separated by SDS-PAGE and transferred to polyvinylidene difluoride membranes. The membranes were blocked by 5% nonfat dry milk in phosphate-buffered saline + 0.05% Tween 20, and subsequently incubated with primary antibodies at 4 ℃ overnight. Next, the membranes were incubated with a peroxidase secondary antibody at room temperature for 1 h. Antibodies and dilutions included the following: anti-nephrin antibody (Abcam, UK, ab216341, 1:1,000), anti-synaptopodin antibody (Novus, Germany, NBP2-39100, 1:500), anti-P-cadherin antibody (Abcam, UK, ab6528, 1:1,000), anti-desmin antibody (Abcam, UK, ab32362, 1:500), FSP-1 antibody (Abcam, UK, ab27957, 1:500), anti-collagen I antibody (Abcam, UK, ab34710, 1:1,000), anti-β-catenin antibody (Abcam, UK, ab32572, 1:1,000), and anti-snail antibody (Abcam, UK, ab180714, 1:1,000). The blots were visualized using LumiGLO reagent and peroxide, followed by exposure to X-ray film. Western blot analyses were performed at least in triplicate.

Reverse transcription polymerase chain reaction (RT-PCR)

Total RNA of the renal cortex and collected podocytes were isolated with TRIzol reagent (Invitrogen, Carlsbad, CA, USA). RNA was then reverse-transcribed into cDNAs by the SuperScript RT kit (Invitrogen) according to the manufacturer's instructions. The relative RNA was detected by SYBR green real-time quantitative reverse transcription PCR (qRTPCR) (Applied Biosystems) and calculated by the $2^{-\Delta\Delta Ct}$ method. The sequences of primers used are displayed in *Table 1*.

Immunofluorescence

Podocytes were cultured on the cover glasses in 12-well plates. The podocytes of different groups as described above were fixed with 4% paraformaldehyde for 30 min. Podocytes were then blocked by 2.5% dunk serum and incubated with primary antibodies for 12 h at 4 ℃. Subsequently, the podocytes were incubated with secondary antibodies at 37 ℃ for 2 h. After counterstaining with DAPI for 5 min, cells were observed under a confocal microscope (Leica TCS SP5 MP, Leica, Heidelberg, Germany). Following antibodies and dilutions were used for the experiments: anti-nephrin antibody (Abcam, UK, ab216341, 1:200), anti-synaptopodin antibody (Novus, Germany, NBP2-39100, 1:200), anti-P-cadherin antibody (Abcam, UK, ab6528,

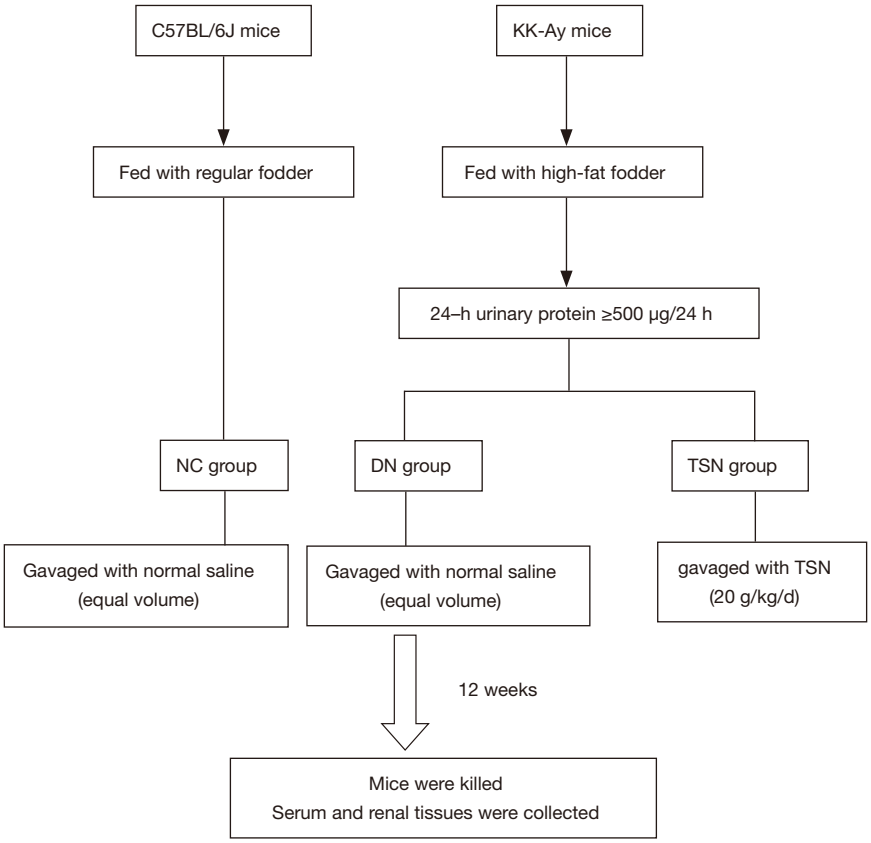

Figure 1 The flow chart of animal experiment. DN, diabetic nephropathy; TSN, Tang-Shen-Ning.

1:200), anti-desmin antibody (Abcam, UK, ab32362, 1:500), anti-FSP-1 antibody (Abcam, UK, ab27957, 1:200), anti-collagen I antibody (Abcam, UK, ab34710, 1:200), anti-β-catenin antibody (Abcam, UK, ab32572, 1:200), and anti-snail antibody (Abcam, UK, ab180714, 1:100).

Phalloidin staining

Podocytes were cultured on the cover glasses in 12-well plates. After the different interventions, the podocytes of different groups were fixed with 4% paraformaldehyde for 30 min. Podocytes were then incubated with phalloidin for 30 min at room temperature. After counterstaining with DAPI for 5 min, cells were observed under a confocal microscope (Leica TCS SP5 MP, Leica, Heidelberg, Germany).

Immunohistochemistry

Renal tissue sections (4 μm) were used for immunohistochemistry, and the process of antigen retrieval was performed for tissue sections. Afterward, primary antibodies were added to renal tissue sections for 24 h at 4 ℃. Then renal tissues were incubated with species-specific secondary antibodies and diaminobenzidine. After counterstaining with hematoxylin, the sections were observed with a fluorescent microscope. Antibodies and dilutions included the following: anti-nephrin antibody (Abcam, UK, ab216341, 1:1,000), anti-synaptopodin antibody (Novus, Germany, NBP2-39100, 1:500), anti-P-cadherin antibody (Abcam, UK, ab6528, 1:500), anti-desmin antibody (Abcam, UK, ab32362, 1:1,000), anti-FSP-1 antibody (Abcam, UK, ab27957, 1:500), and anti-collagen I antibody (Abcam, UK, ab34710, 1:500).

Luciferase reporter assay

Podocytes were incubated with different interventions for 24 h. Afterward, podocytes were transfected with T-cell factor/lymphoid enhancer-binding factor (TCF/LEF) luciferase reporter plasmid by Lipofectamine 2000 (Invitrogen, Carlsbad, CA, USA). At 48 h post-transfection,

cells were lysed and assayed for luciferase activity with a dual-luciferase reporter assay kit (Promega, Madison, WI, USA) on a luminometer (Lumat LB9507). Transfections were performed in triplicate and repeated three times to ensure reproducibility.

Statistical analysis

Data were presented as mean ± SEM. One-way ANOVA was used for statistical analyses. Data was then analyzed by Bonferroni multiple comparison tests for the comparison of more than 2 groups or Student's *t*-test for the comparison of 2 groups. P<0.05 was considered statistically significant.

Results

Characteristics of pure compounds in TSN

Liquid chromatography-mass spectrometry (LC-MS) in both negative and positive ESI modes was performed for substance analysis of TSN. The kinds of substances of TSN were identified by MS. The mass spectrum of the negative base peak and the positive base peaks are displayed in *Figure 2*. Moreover, the identified substances by MS are displayed in *Table 2*. There were 28 kinds of substances identified by MS. Many kinds of substances of TSN such as Puerarin (number 9), Ferulic Acid (number 13), Astragaloside IV (number 24), and Emodin (number 27) might offer the biological activity of ameliorating podocyte injury. Herein, the effect of TSN on the Wnt/β-catenin pathway and podocyte EMT in DN was explored.

Compared with relevant characteristics and health status of mice in three groups

The relevant characteristics of mice was observed before treatment. The weight of mice in three groups has no statistically significant (P>0.05). All mice were responsiveness. The mental state of mice in three groups were normal. No Adverse event was observed after treatment (*Table 3*).

TSN ameliorated proteinuria and improved renal function in diabetic mice

The 24-h urine protein, serum creatinine, and blood urea nitrogen were measured (n=7, 7/10). Our results showed that the 24-h urine protein of the DN and TSN groups were significantly increased as compared with the NC group at the beginning of the intervention. The level of 24-h urine protein of the DN group was gradually increased at 4, 8, and 12 weeks of intervention. Moreover, 24-h urine protein of the TSN group was significantly decreased at 4, 8, and 12 weeks of intervention compared with the DN group (P<0.05) (*Figure 3A*). Compared with the NC group, serum creatinine (Scr), and blood urea nitrogen (BUN) of the DN group were significantly increased. TSN significantly decreased serum creatinine, and BUN of DN mice (P<0.05) (*Figure 3B,3C*). Moreover, renal pathology was observed by HE, PAS, and Masson staining (n=3, 3/10), and the results showed that mesangial matrix was accumulated in the DN group. Compared with the DN group, the accumulation of the mesangial matrix was significantly ameliorated in the TSN group (*Figure 3D*).

TSN improved cell viability and maintained cell cytoskeleton in HG cultured podocyte

The cell viability was detected by CCK-8 in our *in vitro* study. TSN has no effects on cell viability for cultured podocyte in cytotoxicity tests (*Figure 4A*). Moreover, HG significantly decreased cell viability of podocyte. Compared with HG group, the cell viability was significantly increased in high dose TSN group. However, the cell viability was not significantly increased in low dose TSN group and medium dose TSN group compared with HG group (P<0.05) (*Figure 4B*). Herein, the high dose TSN group was considered as TSN group in our further study. Moreover, the podocyte cytoskeleton was observed in our *in vitro* study. The podocyte cytoskeleton was observed as parallel bundles of stress fibers in the NC group. Intracellular actin stress fibers were abolished and replaced by a cortical actin web, resulting in a polygonal cellular shape in the HG group. TSN resumed intracellular actin stress fiber production and maintained the normal cellular shape induced by HG (*Figure 4C*).

TSN increased the epithelial-associated proteins of the podocyte in DN

Podocyte EMT can decrease the epithelial-associated proteins of podocytes such as nephrin, synaptopodin, and P-cadherin in DN. Thus, nephrin, synaptopodin, and P-cadherin protein expressions were detected by western blot, immunohistochemistry, and immunofluorescence *in vivo* and *in vitro* (n=3, 3/10). Our results showed that nephrin, synaptopodin, and P-cadherin protein expressions were significantly decreased in DN mice and high glucose

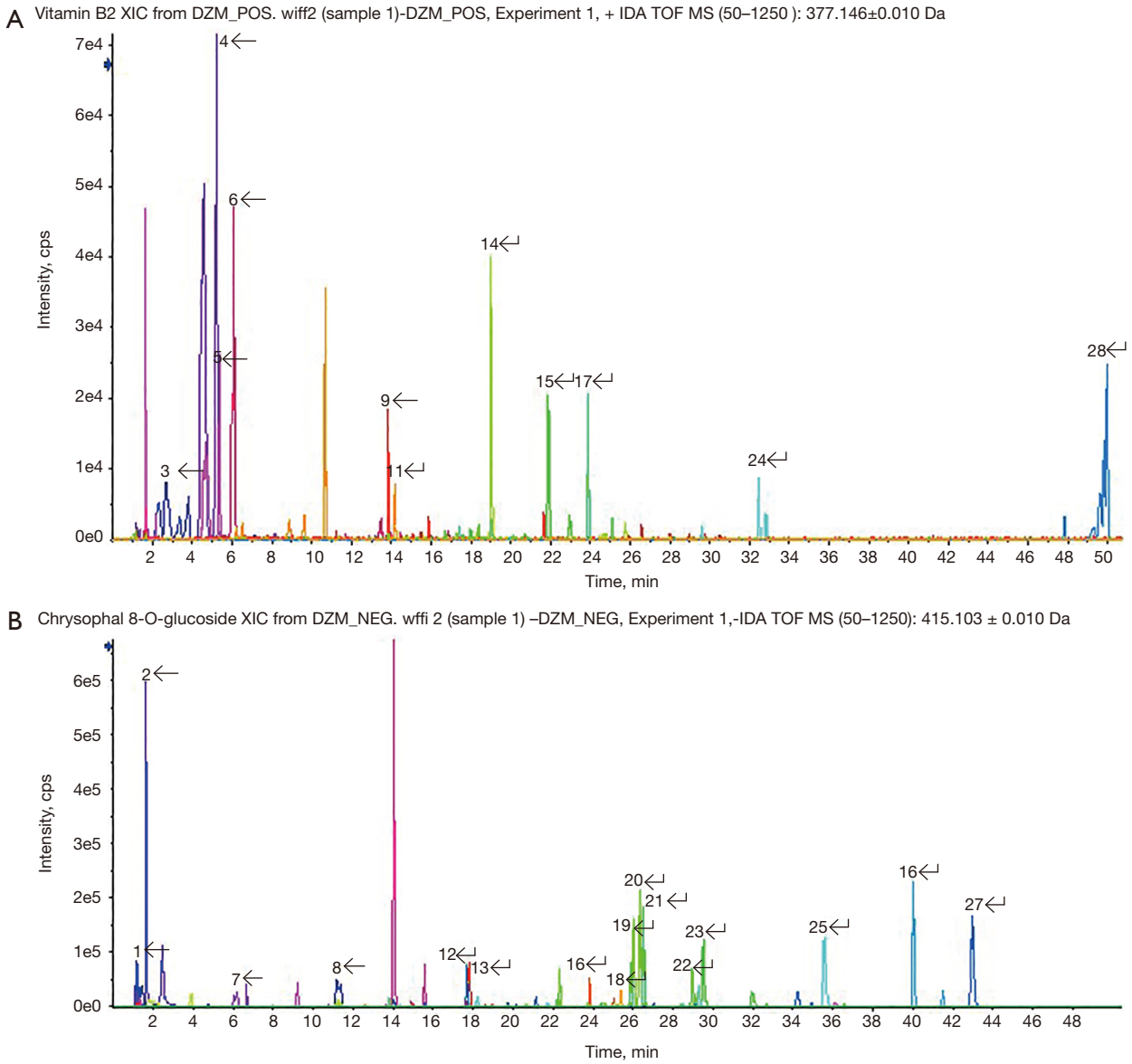

Figure 2 Ion chromatograms of Tang-Shen-Ning (TSN) analyzed by high-performance liquid chromatography-electrospray ionization/mass spectrometry (HPLC-ESI/MSn) analysis. (A) Positive base peak mass spectrometry (MS) spectrum; (B) negative base peak MS spectrum.

cultured podocytes (P<0.05) (*Figure 5A-5F*). The nephrin, synaptopodin, and P-cadherin mRNA expressions were detected by RT-PCR, and the results showed that, as compared with the NC group, nephrin, synaptopodin, and P-cadherin mRNA expressions were significantly decreased in the DN and HG groups. Notably, TSN significantly increased nephrin, synaptopodin, and P-cadherin protein and mRNA expression in DN mice and high glucose cultured podocytes (P<0.05) (*Figure 5G,5H*).

TSN decreased the mesenchymal-associated proteins of the podocyte in DN

Podocytes express proteins of mesenchymal cells, such as desmin, FSP-1 and collagen I, during the process of EMT in DN (n=3, 3/10). Thus, desmin, FSP-1, and collagen I protein expressions were detected by western blot, immunohistochemistry, and immunofluorescence *in vitro*. Our results showed that desmin, FSP-1, and collagen I protein expressions were significantly increased in DN mice

Table 2 Chemical components of TSN identified by HPLC-ESI/MSn

No.	Retention time	Formula	Charge	Precursor mass	Identification
1	1.17	$C_6H_{12}O_6$	[M–H]–	179.0561	D-(+)-glucose
2	1.63	$C_6H_8O_7$	[M–H]–	191.0197	Citric acid
3	2.68	$C_6H_{13}NO_2$	[M+H]+	132.1019	Leucine
4	5.21	$C_{10}H_{13}N_5O_4$	[M+H]+	268.104	Adenosine
5	5.35	$C_{10}H_{13}N_5O_5$	[M+H]+	284.0989	guanosine
6	6.09	$C_9H_{11}NO_2$	[M+H]+	166.0863	Phenprobamate
7	6.15	$C_{27}H_{42}O_{20}$·HCOOH	[M–H]–	731.2251	Rehmannioside D
8	9.21	$C_{11}H_{12}N_2O_2$	[M–H]–	203.0826	L-Tryptophan
9	13.83	$C_{21}H_{20}O_9$	[M+H]+	417.118	Puerarin
10	14.03	$C_{16}H_{22}O_9$·HCOOH	[M–H]–	403.1246	sweroside
11	14.18	$C_{17}H_{20}N_4O_6$	[M+H]+	377.1456	Vitamin B2
12	17.68	$C_{15}H_{10}O_5$	[M–H]–	269.0455	aloe-emodine
13	17.8	$C_{10}H_{10}O_4$	[M–H]–	193.0506	Ferulic Acid
14	19	$C_{21}H_{22}O_9$	[M+H]+	419.1337	Liquiritin
15	21.89	$C_{12}H_{16}O_4$	[M+H]+	225.1121	Senkyunolide I
16	23.82	$C_{31}H_{40}O_{15}$	[M–H]–	651.2294	Rehmannioside
17	23.88	$C_{31}H_{40}O_{15}$·NH_3	[M+H]+	670.2705	Cistanoside D
18	25.39	$C_{23}H_{28}O_{10}$	[M–H]–	463.161	Isomucronulatol-7-O-glucoside
19	25.88	$C_{20}H_{24}O_9$	[M–H]–	407.1348	Torachrysone-8-O-β-D-glucopyranoside
20	26.34	$C_{21}H_{20}O_{10}$	[M–H]–	431.0984	Emodin-8-glucoside
21	29.51	$C_{15}H_{10}O_4$	[M–H]–	253.0506	Chrysophanol
22	26.51	$C_{21}H_{20}O_9$	[M–H]–	415.1035	Chrysophal 8-O-glucoside
23	29.29	$C_{22}H_{22}O_{10}$	[M–H]–	445.114	Physcion-8-O-beta-D-monoglucoside
24	32.46	$C_{41}H_{68}O_{14}$	[M+H]+	785.4682	Astragaloside IV
25	35.57	$C_{15}H_8O_6$	[M–H]–	283.0248	Rhein
26	40.03	$C_{45}H_{72}O_{16}$·HCOOH	[M–H]–	913.4802	Astragaloside I
27	42.99	$C_{15}H_{10}O_5$	[M–H]–	269.0455	Emodin
28	49.96	$C_{24}H_{28}O_4$	[M+H]+	381.206	Senkyunolide O

and high glucose cultured podocyte (P<0.05) (*Figure 6A-6F*). The desmin, FSP-1, and collagen I mRNA expressions were detected by RT-PCR, and the results showed that, as compared with the NC group, desmin, FSP-1, and collagen I mRNA expressions were also significantly increased in the DN and HG groups. More importantly, TSN significantly decreased desmin, FSP-1, and collagen I protein and mRNA expression in DN mice and high glucose cultured podocytes (P<0.05) (*Figure 6G,6H*).

TSN inhibited the activation of the Wnt/β-catenin pathway in podocyte in DN

The Wnt/β-catenin pathway is significantly activated in DN, and the activated Wnt/β-catenin pathway plays a vital role in podocyte EMT (11). Our results showed that β-catenin and Snail expressions were significantly increased in high glucose cultured podocytes. Notably, TSN significantly decreased β-catenin and Snail

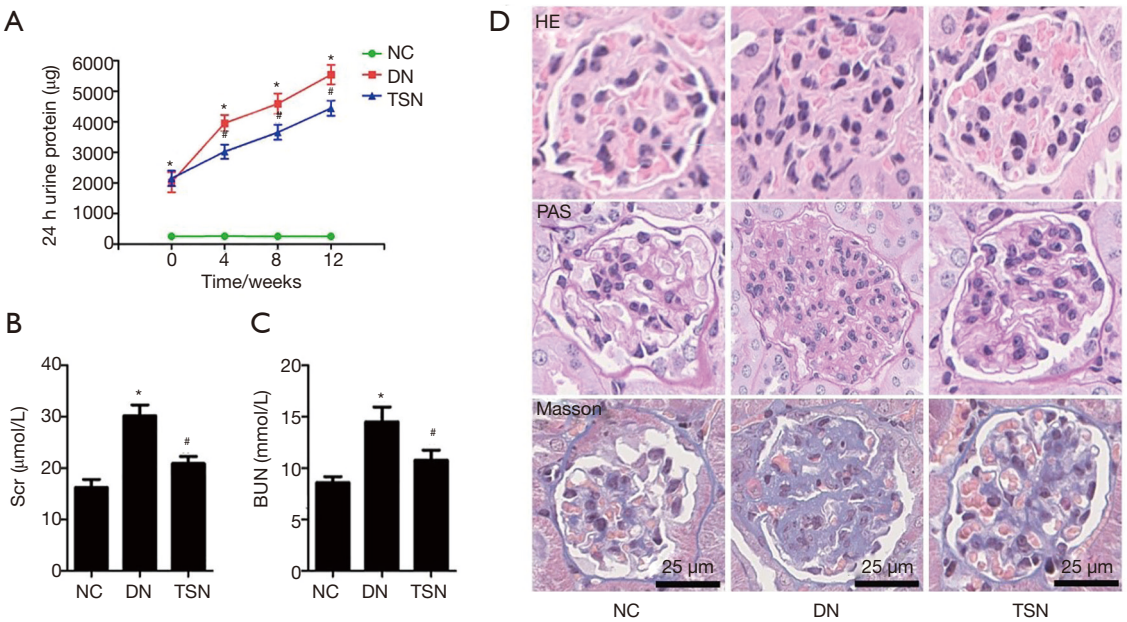

Figure 3 Effects of Tang-Shen-Ning (TSN) on renal function, renal pathology, and podocyte injury in diabetic nephropathy (DN) mice. (A) Comparison of 24-h proteinuria from mice in different groups; (B) comparison of Scr from mice in different groups; (C) comparison of blood urea nitrogen from mice in different groups; (D) representative photographs of HE, PAS, and Masson in different groups. Compared with NC group, *P<0.05; compared with DN/HG group, #P<0.05.

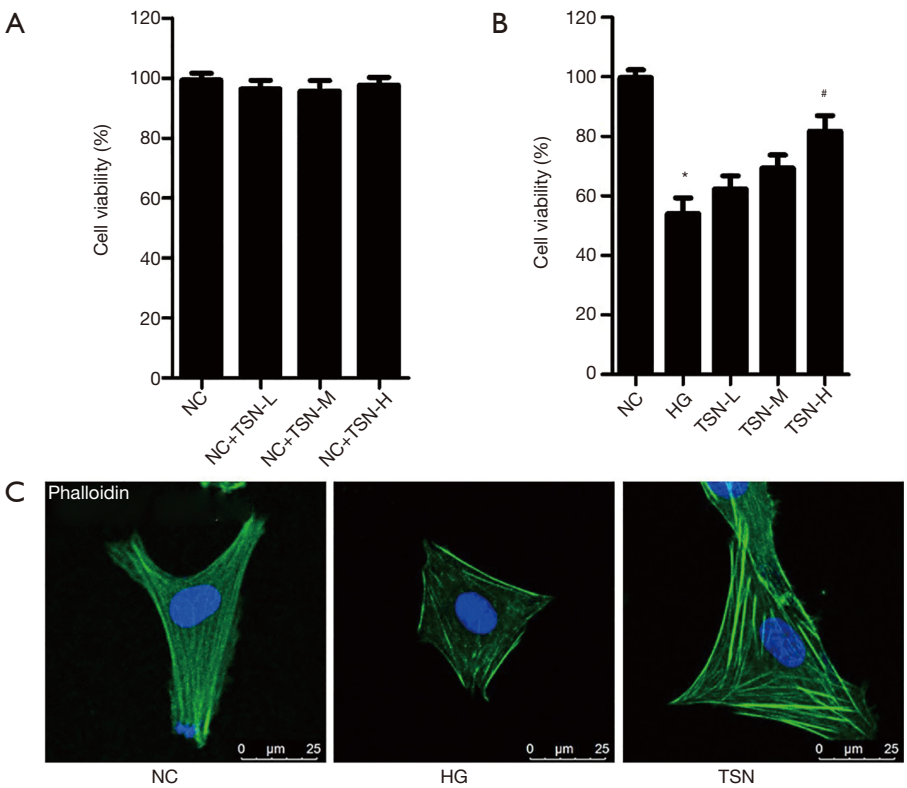

Figure 4 Effects of Tang-Shen-Ning (TSN) on cell viability and cell cytoskeleton in high glucose (HG) cultured podocyte. (A) Comparison of cell cytotoxicity of podocytes in different groups; (B) comparison of cell viability of podocytes in different groups; (C) representative photographs of Phalloidin staining in different groups. Compared with NC group, *P<0.05; Compared with HG group, #P<0.05.

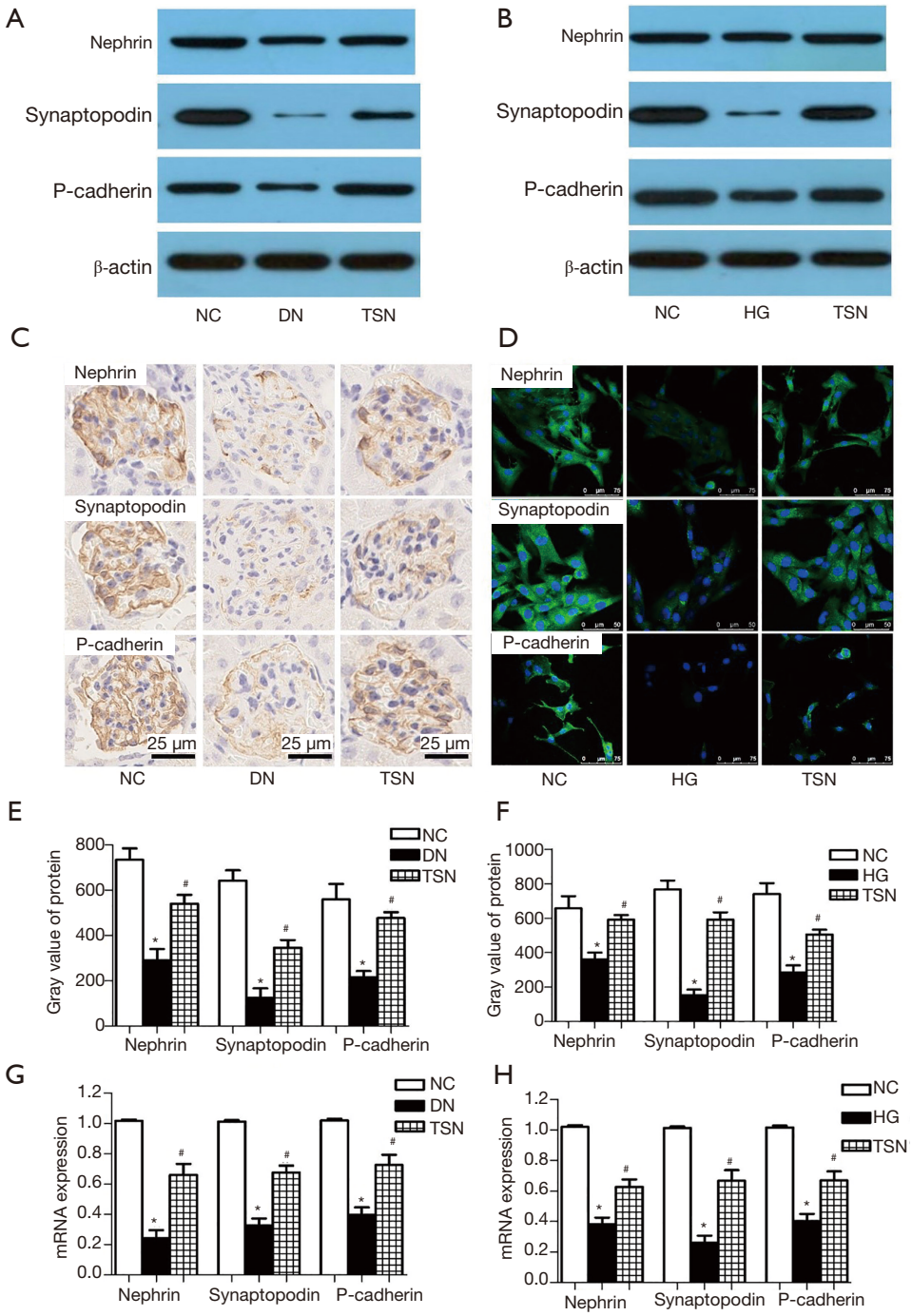

Figure 5 Effects of Tang-Shen-Ning (TSN) on nephrin, synaptopodin, and P-cadherin in podocytes in diabetic nephropathy (DN) mice and high glucose (HG)-cultured podocytes. (A) Representative bands of nephrin, synaptopodin, and P-cadherin in the renal cortex from mice of different groups; (B) representative bands of nephrin, synaptopodin, and P-cadherin in cultured podocytes in different groups; (C) representative photograph of nephrin, synaptopodin, and P-cadherin expression in the renal cortex from mice of different groups (immunohistochemistry); (D) representative photograph of nephrin, synaptopodin, and P-cadherin expression in cultured podocytes in different groups (immunofluorescence); (E) comparison of nephrin, synaptopodin, and P-cadherin protein expression in the mice renal cortex (n=3); (F) comparison of nephrin, synaptopodin, and P-cadherin protein expression in cultured podocytes (n=3); (G) comparison of nephrin, synaptopodin, and P-cadherin mRNA expression in the mice renal cortex (n=3); (H) comparison of nephrin, synaptopodin, and P-cadherin mRNA expression in cultured podocytes (n=3). Compared with NC group, *P<0.05; Compared with DN/HG group, #P<0.05.

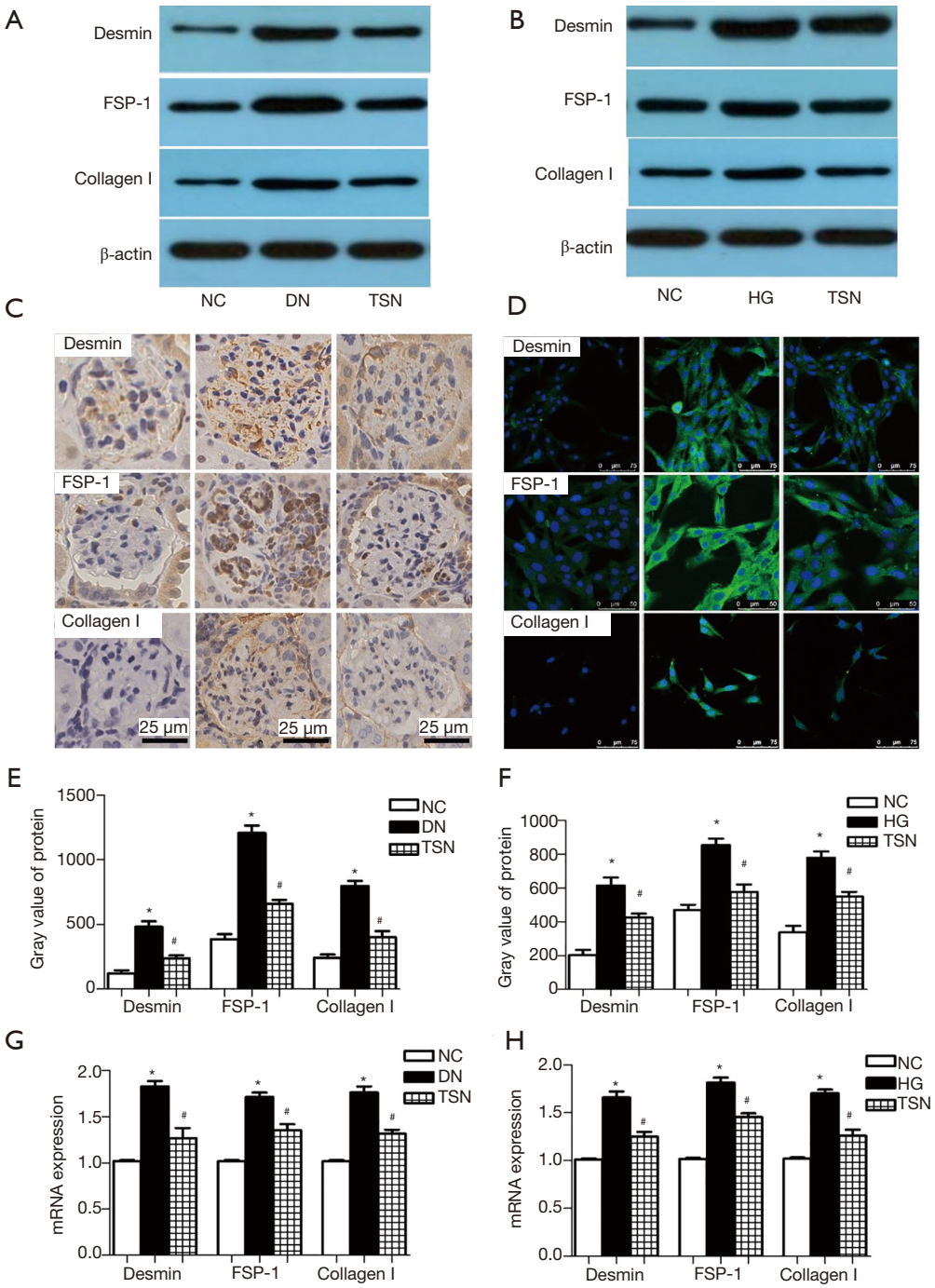

Figure 6 Effects of Tang-Shen-Ning (TSN) on desmin, fibroblast-specific protein 1 (FSP-1), and collagen I in podocytes in diabetic nephropathy (DN) mice and high glucose (HG)-cultured podocytes. (A) Representative bands of desmin, FSP-1, and collagen I in the renal cortex from mice in different groups; (B) representative bands of desmin, FSP-1, and collagen I in cultured podocytes in different groups; (C) representative photograph of desmin, FSP-1, and collagen I expression in the renal cortex from mice in different groups (immunohistochemistry); (D) representative photograph of desmin, FSP-1, and collagen I expression in cultured podocytes in different groups (immunofluorescence); (E) comparison of desmin, FSP-1, and collagen I protein expression in the mice renal cortex (n=3); (F) comparison of desmin, FSP-1, and collagen I protein expression in cultured podocytes (n=3); (G) comparison of desmin, FSP-1, and collagen I mRNA expression in the mice renal cortex (n=3). (H) Comparison of desmin, FSP-1, and collagen I mRNA expression in cultured podocytes (n=3). Compared with NC group, *P<0.05; Compared with DN/HG group, #P<0.05.

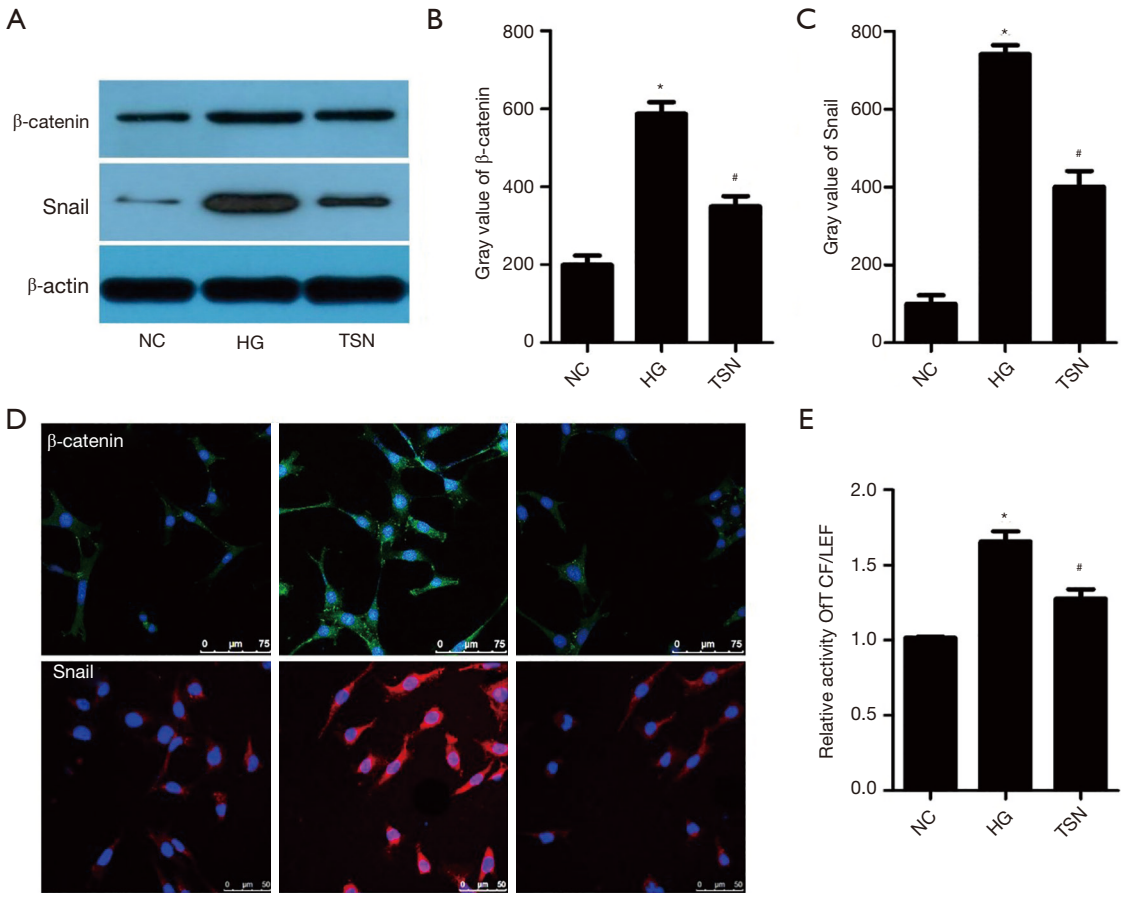

Figure 7 Effects of Tang-Shen-Ning (TSN) on the Wnt/β-catenin pathway in high glucose (HG)-cultured podocytes. (A) Representative bands of β-catenin and Snail in cultured podocytes in different groups; (B) comparison of β-catenin protein in cultured podocytes in different groups (n=3); (C) comparison of Snail protein in cultured podocytes in different groups (n=3); (D) representative photograph of β-catenin and Snail expression in cultured podocytes in different groups (immunofluorescence); (E) relative activity of TCF/LEF detected by luciferase reporter assay in different groups (n=3). Compared with NC group, *P<0.05; Compared with DN/HG group, #P<0.05.

expression in high glucose cultured podocytes (P<0.05) (*Figure 7A-7D*). Moreover, the activity of TCF/LEF was detected by a luciferase reporter assay, and the results showed that the TCF/LEF activity was significantly increased in the HG group. Meanwhile, TSN significantly decreased the TCF/LEF activity of HG cultured podocyte (P<0.05) (*Figure 7E*).

Activation of the Wnt/β-catenin pathway reversed the effect of TSN on podocyte EMT

To detect the role of the Wnt/β-catenin pathway on podocyte EMT, CTNNB1^{Ko} and CTNNB1^{Ki} were transfected in podocytes, respectively. To confirm transfection, β-catenin protein expression was detected, and the results showed that CTNNB1^{Ko} transfection significantly decreased β-catenin expression of podocytes. Moreover, CTNNB1^{Ki} transfection significantly increased the β-catenin expression of podocytes (P<0.05) (*Figure 8A-8C*). Snail, an important target gene of β-catenin, was detected in different groups, and an increased expression of Snail by HG was reversed by CTNNB1^{Ko} transfection. Meanwhile, the decreased expression of Snail by TSN was reversed by CTNNB1^{Ki} transfection. FSP-1 and P-cadherin are the mesenchymal-associated and epithelial-associated proteins of the podocyte, respectively. Thus, FSP-1 and P-cadherin expression were also detected after transfection. Similarly, the increased expression of FSP-1 and decreased expression of P-cadherin by HG was reversed by CTNNB1^{Ko} transfection. The decreased expression of FSP-1 and

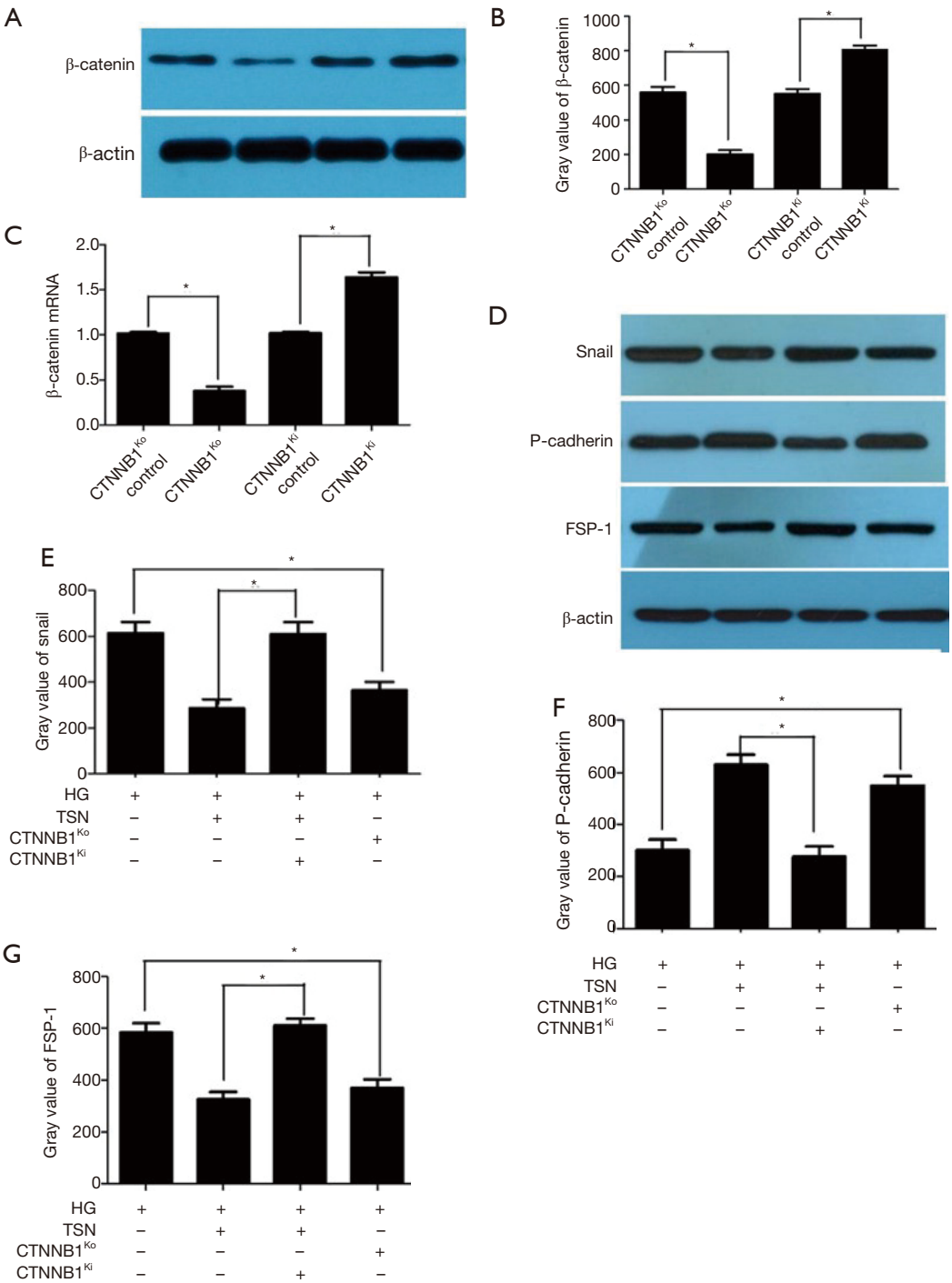

Figure 8 Effects of CTNNB1Ko and CTNNB1Ki on podocyte epithelial-esenchymal transformation (EMT) in the cultured podocytes. (A) Representative β-catenin protein bands in cultured podocytes in CTNNB1Ko and CTNNB1Ki groups; (B) comparison of β-catenin protein in cultured podocytes in CTNNB1Ko and CTNNB1Ki groups (n=3); (C) comparison of β-catenin mRNA in cultured podocytes in CTNNB1Ko and CTNNB1Ki groups (n=3); (D) representative bands of Snail, P-cadherin, and fibroblast-specific protein 1 (FSP-1) protein in cultured podocytes in different groups; (E) comparison of Snail protein in cultured podocytes in different groups (n=3); (F) comparison of P-cadherin protein in cultured podocytes in different groups (n=3); (G) comparison of FSP-1 protein in cultured podocytes in different groups (n=3). *P<0.05.

Table 3 Relevant characteristics and health status of mice

Group	Weight (g)	Responsiveness	Mental state
NC	21.32±2.31	Normal	Normal
Diabetic nephropathy (DN)	22.46±2.82	Normal	Normal
Tang-Shen-Ning (TSN)	21.76±1.95	Normal	Normal

NC, normal control.

increased expression of P-cadherin by TSN was reversed by $CTNNB1^{Ki}$ transfection (P<0.05) (*Figure 8D-8G*).

Discussion

DN is the main cause of ESRD (1). However, the exact mechanism of DN is unclear. Moreover, clinical treatments have not effectively delayed the progression of DN (17). Thus, new therapeutic targets and drugs are urgently needed for DN patients. It has been demonstrated that proteinuria is the major biochemical feature and important risk factor for the progression of DN (18). The glomerular filtration barrier (GFB), composed of three major layers, plays a key role in proteinuria in DN (19). Podocytes, the most important structures of GFB, can be injured by hyperglycemia and oxidant stress in DN. Podocyte injury can induce destruction of GBM and increased urinary albumin. Therefore, podocyte injury, as the key pathological mechanism of DN, has been the research focus and important potential therapeutic target of DN (2-4). TCM compounds can provide preventive and curative delays in the progression of diabetes and its complications (13-15). TSN formula is a natural herbal medicine formulated based on the empirical experience of a Chinese medicine expert, Yan-Bin Gao. TSN has been shown to decrease proteinuria and delay the progression of DN in our clinical practice. The substances of TSN have been analyzed by MS in our study. The substances of TSN such as puerarin (20), Ferulic acid (21), Astragaloside IV (16), and Emodin (22) have been shown to ameliorate podocyte injury in previous studies. Therefore, the effect of TSN on proteinuria and podocyte injury in DN was explored. In our study, TSN exhibited a therapeutic effect on diabetic mice. TSN significantly decreased the level of 24-h urinary protein, serum creatinine, and BUN in KK-Ay mice. Meanwhile, TSN ameliorated renal ultrastructural changes of KK-Ay mice. Notably, TSN ameliorated podocyte foot efface, inhibited podocyte apoptosis, and protected podocytes from injury. KK-Ay mice have been a useful spontaneous animal model for the evaluation of pathogenesis and treatment in patients with type 2 DN in recent years. Herein the molecular mechanism of TSN in DN needed to be explored.

EMT is a process that epithelial cells lose their hallmark epithelial characteristics and gain the features of mesenchymal cells. Podocyte is a kind of visceral epithelial cell. However, podocyte also undergo phenotypic conversion in many chronic kidney diseases. Previous studies have demonstrated that HG can induce podocyte EMT, which plays a critical role in the progression of DN (23). Podocyte EMT is a process that can induce podocyte loss of epithelial characteristics and gain the features of mesenchymal cells. It has been demonstrated that podocyte EMT decreases slit diaphragm-associated proteins, such as nephrin, synaptopodin, and P-cadherin (6). Podocytes express proteins of mesenchymal cells, such as desmin, FSP-1, and collagen I, during the process of EMT (6). Finally, podocyte EMT can induce actin cytoskeleton rearrangement and slit diaphragm loss (24). Therefore, inhibition of podocyte EMT may be a key therapeutic method for many chronic kidney diseases, including DN (25,26). As TSN protected podocytes from injury, the effect of TSN on podocyte EMT was explored in our *in vivo* and *in vitro* studies. In our study, TSN significantly increased nephrin, synaptopodin, P-cadherin expression and decreased desmin, FSP-1, and collagen I expression of podocyte in DN. Thus, TSN significantly ameliorated podocyte EMT induced by HG *in vivo* and *in vitro*.

There is growing evidence that the activation of Wnt/β-catenin pathway is involved in podocyte EMT. Previous studies have demonstrated that Wnt/β-catenin of podocytes can be activated by HG (11,27). The activation of Wnt/β-catenin pathway induces a series of downstream signaling events and finally lead to the dephosphorylation of β-catenin. Dephosphorylated β-catenin is then translocated to the nuclei and bound to TCF/LEF transcription factors (28-30). Snail, an important target gene of β-catenin, is significantly

increased after the activation of Wnt/β-catenin pathway (31). Meanwhile, Snail plays a key role in regulating podocyte EMT. Increased Snail expression can induce up-regulation of desmin, FSP-1, and collagen I and down-regulation of nephrin, synaptopodin, and P-cadherin (12). Therefore, inhibition Wnt/β-catenin pathway could be an effective means to ameliorate podocyte EMT in DN. In our study, β-catenin, TCF/LEF, and Snail were detected *in vivo* and *in vitro*, and Wnt/β-catenin was significantly activated in DN, which has been demonstrated by a previous study (32). More importantly, TSN significantly inhibited the activation of Wnt/β-catenin pathway *in vivo* and in vitro. To confirm the relationship of the Wnt/β-catenin pathway and podocyte EMT, $CTNNB1^{Ko}$ and $CTNNB1^{Ki}$ was transfected into cultured podocytes. Indeed, podocyte EMT induced by HG could be reversed via treatment of $CTNNB1^{Ko}$. Meanwhile, the effect of TSN on podocyte EMT could be reversed by $CTNNB1^{Ki}$ in HG cultured podocyte.

Conclusions

In our study, TSN significantly decreased proteinuria and improved renal function in DN. Moreover, TSN significantly inhibited the activation of Wnt/β-catenin pathway and ameliorated podocyte EMT. More importantly, the activation of Wnt/β-catenin pathway by $CTNNB1^{Ki}$ significantly reversed the effect of TSN on podocyte EMT. Herein, we speculated that TSN might have pleiotropic effect on Wnt/β-catenin pathway in podocyte, which may be a main mechanism of protected effect on podocyte EMT in DN. However, the other therapeutic target of TSN on podocyte injury in DN remains unclear. Thus, further studies will be performed in our later research.

Acknowledgments

Funding: This work was supported by grants from the National Natural Science Foundation of China (No. 81703989) and the Beijing Natural Science Foundation (No. 7182069 and 7172096).

Footnote

Provenance and Peer Review: This article was commissioned by the Guest Editors (Bo Li and Lyubima Despotova-Toleva) for the focused series "Narrative & Evidence-based Medicine for Traditional Medicine: from basic research to clinical practice and trial" published in *Annals of Palliative Medicine*. The article has undergone external peer review.

Reporting Checklist: The authors have completed the ARRIVE reporting checklist. Available at http://dx.doi.org/10.21037/apm-20-602

Data Sharing Statement: Available at http://dx.doi.org/10.21037/apm-20-602

Peer Review File: Available at http://dx.doi.org/10.21037/apm-20-602

Conflicts of Interest: All authors have completed the ICMJE uniform disclosure form (available at http://dx.doi.org/10.21037/apm-20-602). The series "Narrative & Evidence-based Medicine for Traditional Medicine: from basic research to clinical practice and trial" was commissioned by the editorial office without any funding sponsorship. The authors have no other conflicts of interest to declare.

Ethical Statement: The authors are accountable for all aspects of the work in ensuring that questions related to the accuracy or integrity of any part of the work are appropriately investigated and resolved. The study was approved by the Medical Ethics Committee of Capital Medical University (No. AEEI-2018-073). Our animal experiment was performed following the National Institutes of Health Guide for the Care and Use of Laboratory Animals.

References

1. Ahmad J. Management of diabetic nephropathy: Recent progress and future perspective. Diabetes Metab Syndr 2015;9:343-58.
2. Zhao SM, Zhang T, Qiu Q, et al. MiRNA-337 leads to

podocyte injury in mice with diabetic nephropathy. Eur Rev Med Pharmacol Sci 2019;23:8485-92.
3. Wang T, Gao Y, Wang X, et al. Calpain-10 drives podocyte apoptosis and renal injury in diabetic nephropathy. Diabetes Metab Syndr Obes 2019;12:1811-20.
4. Ji J, Zhao Y, Na C, et al. Connexin 43-autophagy loop in the podocyte injury of diabetic nephropathy. Int J Mol Med 2019;44:1781-8.
5. Bhatti AB, Usman M. Drug Targets for Oxidative Podocyte Injury in Diabetic Nephropathy. Cureus 2015;7:e393.
6. Li Y, Kang YS, Dai C, et al. Epithelial-to-mesenchymal transition is a potential pathway leading to podocyte dysfunction and proteinuria. Am J Pathol 2008;172:299-308.
7. Sedor JR, Madhavan SM, Kim, JH, et al. Out on a LIM: chronic kidney disease, podocyte phenotype and the Wilm's tumor interacting protein (WTIP). Trans Am Clin Climatol Assoc 2011;122:184-97.
8. Zavadil J, Bottinger EP. TGF-β and epithelial-to-mesenchymal transitions. Oncogene 2005;24:5764-74.
9. Kang YS, Li Y, Dai C, et al. Inhibition of integrin-linked kinase blocks podocyte epithelial-mesenchymal transition and ameliorates proteinuria. Kidney Int 2010;78:363-73.
10. Neilson EG. Mechanisms of disease: Fibroblasts—A new look at an old problem. Nat Clin Pract Nephrol 2006;2:101-8.
11. Dai C, Stolz DB, Kiss LP, et al. Wnt/beta-catenin signaling promotes podocyte dysfunction and albuminuria. J Am Soc Nephrol 2009;20:1997-2008.
12. Matsui I, Ito T, Kurihara H, et al. Snail, a transcriptional regulator, represses nephrin expression in glomerular epithelial cells of nephrotic rats. Lab Invest 2007; 87: 273–283.
13. Tong XL, Dong L, Chen L, et al. Treatment of diabetes using traditional Chinese medicine: past, present and future. Am J Chin Med 2012;40:877-86.
14. Shi X, Lu XG, Zhan LB, et al. The effects of the Chinese medicine ZiBu PiYin recipe on the hippocampus in a rat model of diabetes-associated cognitive decline: a proteomic analysis. Diabetologia 2011;54:1888-99.
15. Wen X, Zeng Y, Liu L, et al. Zhenqing recipe alleviates diabetic nephropathy in experimental type 2 diabetic rats through suppression of SREBP-1c. J Ethnopharmacol 2012;142:144-50.
16. Wang X, Gao Y, Tian N, et al. Astragaloside IV improves renal function and fibrosis via inhibition of miR-21-induced podocyte dedifferentiation and mesangial cell activation in diabetic mice. Drug Des Devel Ther 2018;12:2431-42.
17. A/L B Vasanth Rao VR, Rao VR, Tan SH, et al. Diabetic nephropathy: An update on pathogenesis and drug development. Diabetes Metab Syndr 2019;13:754-62.
18. Jain A, Nahata A, Lodhi S, et al. Effects of Tephrosia purpurea and Momordica dioica on streptozotocin-induced diabetic nephropathy in rats. Biomed Prev Nutr 2014;4:383-9.
19. Jarad G, Miner JH. Update on the glomerular filtration barrier. Curr Opin Nephrol Hypertens 2009;18:226-32.
20. Li X, Cai W, Lee K, et al. Publisher Correction: Puerarin attenuates diabetic kidney injury through the suppression of NOX4 expression in podocytes. Sci Rep 2018;8:4294.
21. Choi R, Kim BH, Naowaboot J, et al. Effects of ferulic acid on diabetic nephropathy in a rat model of type 2 diabetes. Exp Mol Med 2011;43:676-83.
22. Chen T, Zheng LY, Xiao W, et al. Emodin ameliorates high glucose induced-podocyte epithelial-mesenchymal transition in-vitro and in-vivo. Cell Physiol Biochem 2015;35:1425-36.
23. Yamaguchi Y, Iwano M, Toyoda M, et al. Epithelial-mesenchymal transition as an explanation for podocyte depletion in diabetic nephropathy. Am J Kidney Dis 2009;54:653-64.
24. Valcourt U, Kowanetz M, Niimi H, et al. TGF-beta and the Smad signaling pathway support transcriptomic reprogramming during epithelial-mesenchymal cell transition. Mol Biol Cell 2005;16:1987-2002.
25. Liu Y. Hepatocyte growth factor in kidney fibrosis: Therapeutic potential and mechanisms of action. Am J Physiol Renal Physiol 2004;287:F7-16.
26. Li Y, Tan X, Dai C, et al. Inhibition of integrin-linked kinase attenuates renal interstitial fibrosis. J Am Soc Nephrol 2009;20:1907-18.
27. Liu Y. New insights into epithelial-mesenchymal transition in kidney fibrosis. J Am Soc Nephrol 2010;21:212-22.
28. Moon RT, Kohn AD, De Ferrari GV, et al. WNT and beta-catenin signaling: diseases and therapies. Nat Rev Genet 2004;5:691-701.
29. Huang H, He X. Wnt/beta-catenin signaling: New (and old) players and new insights. Curr Opin Cell Biol 2008;20:119-25.
30. White BD, Nguyen NK, Moon RT. Wnt signaling: It gets more humorous with age. Curr Biol 2007;17:R923-5.
31. He W, Kang YS, Dai C, et al. Blockade of Wnt/β-catenin signaling by paricalcitol ameliorates proteinuria and kidney injury. J Am Soc Nephrol 2011;22:90-103.
32. Li Z, Xu J, Xu P, et al. Wnt/β-catenin signalling pathway mediates high glucose induced cell injury through activation of TRPC6 in podocytes. Cell Prolif 2013;46:76-85.

Cite this article as: Cui FQ, Gao YB, Wang YF, Meng Y, Cai Z, Shen C, Jiang XC, Zhao WJ. Effect of Tang-Shen-Ning decoction on podocyte epithelial-esenchymal transformation via inhibiting Wnt/β-catenin pathway in diabetic mice. Ann Palliat Med 2021;10(12):12921-12936. doi: 10.21037/apm-20-602

